



Aberystwyth University

The responding and ecological contribution of biofilm-leaves of submerged macrophytes on phenanthrene dissipation in sediments

Zhao, Zhenhua; Qin, Zhirui; Xia, Liling; Zhang, Dan; Mela, Sara; Li, Yong

Published in:
Environmental Pollution

DOI:
[10.1016/j.envpol.2018.12.030](https://doi.org/10.1016/j.envpol.2018.12.030)

Publication date:
2019

Citation for published version (APA):

Zhao, Z., Qin, Z., Xia, L., Zhang, D., Mela, S., & Li, Y. (2019). The responding and ecological contribution of biofilm-leaves of submerged macrophytes on phenanthrene dissipation in sediments. *Environmental Pollution*, 246, 357-365. <https://doi.org/10.1016/j.envpol.2018.12.030>

Document License CC BY-NC-ND

General rights

Copyright and moral rights for the publications made accessible in the Aberystwyth Research Portal (the Institutional Repository) are retained by the authors and/or other copyright owners and it is a condition of accessing publications that users recognise and abide by the legal requirements associated with these rights.

- Users may download and print one copy of any publication from the Aberystwyth Research Portal for the purpose of private study or research.
- You may not further distribute the material or use it for any profit-making activity or commercial gain
- You may freely distribute the URL identifying the publication in the Aberystwyth Research Portal

Take down policy

If you believe that this document breaches copyright please contact us providing details, and we will remove access to the work immediately and investigate your claim.

tel: +44 1970 62 2400
email: is@aber.ac.uk

1 **The responding and ecological contribution of biofilm-leaves**
2 **of submerged macrophytes on phenanthrene dissipation in**
3 **sediments**

4 Zhenhua Zhao^{1,2*}, Zhirui Qin¹, liling Xia³, Dan Zhang¹, Sara Margaret Mela⁴, Yong Li¹

5 ¹ Key Laboratory of Integrated Regulation and Resource Development on Shallow Lake
6 of Ministry of Education, College of Environment, Hohai University, Nanjing 210098,
7 P.R. China.

8 ² Department of Plant, Soil, and Microbial Sciences, Michigan State University, East
9 Lansing, MI 48824, USA.

10 ³ Nanjing Institute of Industry Technology, Nanjing 210016, P.R. China

11 ⁴ Department of Geography and Earth Sciences, Aberystwyth University, Penglais,
12 Aberystwyth, Ceredigion, SY23 3DB, UK

13
14
15 *Corresponding author: E-mail: zzh4000@126.com (Zhenhua Zhao)

16 Tel.: +86 25 83786696; Fax: +86 25 83786696

17

18 **Abstract**

19 The bacterial communities and ecological contribution of biofilm-leaves of the
20 *Vallisneria natans* (VN), *Hydrilla verticillata* (HV) and artificial plant (AP) settled in
21 sediments with different polluted levels of phenanthrene were investigated by high-
22 throughput sequencing in different growth periods. There was no significant difference
23 among the detected Alpha diversity indices based on three classification, attached surface,
24 spiking concentration and incubation time. While Beta diversity analysis assessed by
25 PCoA on operational taxonomic units (OTU) indicated that bacterial community
26 structures were significantly influenced in order of attached surface > incubation time >
27 spiking concentration of phenanthrene in sediment. Moreover, the results of hierarchical
28 dendrograms and heat maps at genus level were consistent with PCoA analysis. We
29 speculated that the weak influence of phenanthrene spiking concentration in sediment
30 might be related to lower concentration and smaller concentration gradient of
31 phenanthrene in leaves. Meanwhile, difference analysis suggested that attached surface
32 was inclined to influence the rare genera up to significant level than incubation time. In
33 general, the results proved that phenanthrene concentrations, submerged macrophytes
34 categories and incubation time did influence the bacterial community of biofilm-leaves.
35 In turn, results also showed a non-negligible ecological contribution of biofilm-leaves in
36 dissipating the phenanthrene in sediments (>13.2%-17.1%) in contrast with rhizosphere
37 remediation (2.5%-3.2% for HV and 9.9%-10.6% for VN).

38

39 Capsule: The bacterial community structures were influenced in order of attached surface >

40 incubation time > spiking concentration of phenanthrene in sediment.

41

42 **Key words:** phenanthrene bioremediation; submerged macrophyte; biofilm-leaf;

43 bacterial community; high-throughput sequencing

44

45 **1. Introduction**

46 Polycyclic aromatic hydrocarbons (PAHs) are widely distributed environmental
47 pollutants (Chen et al., 2015; Li et al., 2014), which result from incomplete combustion
48 of fossil fuels and organic materials, and are often associated with industrial and human
49 activities (Bamforth and Singleton, 2010). PAHs are highly carcinogenic, teratogenic and
50 mutagenic compounds and can pose a great threat to human health through food-chain
51 bioaccumulation (Moscoso et al., 2012). As demonstrated by studies on occurring,
52 transporting, adsorbing and biodegrading, the concentrations of PAHs in natural
53 environments can be detected in a wide scope from 1 ng/g to 300 mg/kg (Lu et al., 2012).
54 PAHs typically precipitate and accumulate in sediments due to their hydrophobic
55 properties in aquatic environment (Liang et al., 2007; Wang et al., 2003), which result in
56 the sediment being the major sink of PAHs. Meanwhile, several studies indicate that
57 sediments may be the second-most concentrated source of PAHs (Jérôme Cachot et al.,
58 2007; Yang et al., 2008). PAHs observed in sediments mainly consist of 3-rings PAHs
59 (e.g. phenanthrene) and 4-rings PAHs (e.g. pyrene) (Hassan et al., 2018; Lin et al., 2016).
60 Dredging contaminated sediments is a common but disruptive practice which can lead to
61 the re-suspension of pollutants (Agarwal et al., 2007). Therefore, exploring cost-effective,
62 in situ approaches for sediment remediation has become increasingly important (Perelo,
63 2010).

64 Phytoremediation is a prospective alternative means because of its affordability,
65 effectiveness and low environmental impact (Cheema et al., 2010; Gomes et al., 2013). A
66 considerable amount of work has been done investigating the rhizosphere, which could

67 improve microbial population and diversity of soil surrounding plant roots (Ma et al.,
68 2010). Such studies mainly focus on the rhizosphere of terrestrial plants, while submerged
69 plants are the key and widespread species in coastal shallow water. Diverse microbiomes
70 were often associated with submerged rhizoplanes, due to the unique environment that
71 persists compared to their terrestrial counterparts (Srivastava et al., 2016; Zhao et al.,
72 2017). This plant-microbes ecosystem could be manipulated to alleviate the condition of
73 polluted sediments naturally. The high root oxygen loss (ROL) capacity of submerged
74 macrophytes could contribute to nitrogen cycling in sediments: higher abundance of
75 ammonia oxidizers increased denitrification, while nitrifies and denitrifying communities
76 may associate more closely in these environments (Vila - Costa et al., 2016).

77 Recently, the remediation strategy of using submerged macrophytes to deal with
78 sediments polluted by PAHs has attracted widespread attention. Meng et al. (2015)
79 showed that microbial degradation, rather than plant uptake, played a major role in the
80 plant-promoted the dissipation of PAHs in sediments, and microbial degradation was not
81 controlled by the amount of bioavailable PAHs - even if these were readily bioavailable.
82 Dissipation ratio of PAHs was correlated with PAH-degrading bacteria population which
83 in turn, linked positively with sediment redox potential, and low plant density of
84 *Vallisneria spiralis* should be a better selection for phytoremediation (Liu et al., 2014). In
85 addition, *Potamogeton crispus* greatly improved the bioavailability (73.9%) and
86 biodegradation activity (277%) of pyrene in aged sediments in contrast with unaged
87 sediments (13.1% and 150%, respectively) (Meng and Chi, 2016).

88 Diverse substances such as organic matter, silt, zoogloea, algae and other
89 microorganisms often accumulate on the leaf surface of submerged plants. A micro-
90 interface is therefore established which varies in its composition, structure and thickness
91 depending on the actual environmental properties. This impacts the gas exchange between
92 water and plants and induces specific heterogeneous oxidation – reduction environments.
93 Numerous investigations have focused on the micro-interface of submerged macrophytes.
94 Sand-Jensen et al. (1985) reported that dissolved oxygen (DO) on the micro-interfaces of
95 leaves of *Potamogeton crispus*, *Littorella uniflora*, *Zostera marina* and *Scytosiphon*
96 *lomentaria* increased with shorter distance from the leaf surfaces, and with increasing
97 illumination intensity. In the daytime, the leaf surfaces of submerged macrophytes
98 produced an oxygen-enriched environment, while a highly anaerobic environment
99 appeared in night. Meanwhile, the pH in the micro-interfaces was greater than
100 surrounding water (Jones et al., 2000; Sandjensen et al., 1985), and the difference value
101 increased with the thickness of biofilm (Jones et al., 2000). Recently, high throughput
102 sequencing, and next generation sequencing technology has provided gene sequence
103 outputs that could be further analyzed to provide in-depth bacterial taxonomic
104 assignments (Kim and Isaacson, 2015). Thus, some researchers studied the response and
105 role of functional bacteria on biofilm-leaves for eutrophication, especially for nitrogen in
106 aquatic environments through high throughput sequencing technology (Pang et al., 2016;
107 Yan et al., 2017; Zhang et al., 2016). Little is known about the cumulative capacity of
108 PAHs in the leaves of submerged macrophytes and their impact on the biofilm-leaves

109 when they release from sediments to water due to the characterization of hydrophobicity
110 normally. However, Lipotropy of leaves of submerged plants makes them enrich PAHs
111 from water (Diepens et al., 2014). PAHs may be mediated by microorganisms in micro-
112 interfaces, especially bacteria. Thus, we hypothesized that the bacterial community in
113 biofilm attached on leaves of submerged macrophytes suffering from PAHs might be
114 altered and biofilm-leaves might contribute to the dissipation of PAHs in turn.

115 In our present study, phenanthrene was chosen as one of representative low molecular
116 weight (LMW) PAHs because it is commonly found in sediments. The bacterial
117 community and ecological contribution of biofilm-leaves were identified by high
118 throughput sequencing, compared between an artificial plant and two submerged
119 macrophytes in different growth periods, settled in sediments spiked with different
120 phenanthrene concentrations. The objective of this study is to explore and identify the key
121 driving factor influencing the bacterial community of biofilm-leaves and the ecological
122 contribution of different dissipation mechanism (e.g. biofilm, submerged macrophytes,
123 and background degradation) on phenanthrene dissipation in water and sediment.

124 **2. Materials and methods**

125 *2.1 Materials*

126 *Vallisneria natans* (VN) and *Hydrilla verticillata* (HV) (Nanjing Sam Creek aquatic
127 breeding research base) were selected as the tested aquatic plants. A control group (CG)
128 and artificial plants group (bio-racks with organic glass, AP) with similar surface area to
129 submerged macrophytes were also tested. Sediments (pH=7.32, organic matter=2.14%,

130 background phenanthrene level=0.056 mg/kg) were collected from a suburb river of
131 Nanjing (not in the main industrial area), air-dried, manually crushed, and then sieved
132 with 2-mm mesh to remove plant residues and stone. Organic glass containers (40 × 50
133 cm) were chosen to cultivate submerged plants, to avoid loss of phenanthrene via
134 adsorption. The experiment was carried out in the ecological greenhouse with three
135 replicates for 35 d.

136 *2.2 Experimental setup*

137 The 0.6 g phenanthrene dissolved in acetone (1600 mL) was spiked into 6 kg sediment.
138 After acetone evaporating, the polluted sediment was mixed with unpolluted sediment
139 with their respective proportion, and laid in each container smoothly. The final contents
140 of phenanthrene in sediment (dry weight) were 20 mg/kg and 10 mg/kg, respectively.

141 0.01 g norfloxacin and 0.015 g roxithromycin / L water) were added into water to
142 domesticate for 3 – 5 d, which could remove or destroy the original biofilm-leaves. After
143 the completion of plant domestication, the robust and uniform plants were transplanted
144 into the containers. 50 L water was added to the container and the water-line was marked
145 clearly to replenish water to a uniform level throughout cultivation.

146 Water, leaf and sediment samples were collected for phenanthrene analysis at 14, 28
147 and 35 d. The samples were stored at -20°C for PAHs analysis. The biofilm-leaves of
148 submerged plants and biofilm-surface of AP were extracted in 14 and 28 d, respectively.

149 *2.3 The separation of biofilm attached on the plants leaves*

150 The method of biofilm separation from leaf surfaces was modified from He et al. (2012).

151 With precool ethanol-PBS buffer as eluent, appropriate amount of leaves were put in the
152 polyethylene test tube, then Triton solution and several 3 mm glass beads were added. All
153 the sample tubes were placed in reciprocating oscillator with constant temperature and
154 were shaken for 10 min (225 r/min), then underwent ultrasounds (150 W, 40 kHz) for 1
155 min. After filtrating elution liquor, the filtrate was centrifuged for 10 min (10000 rpm),
156 and the centrifugal precipitate was collected. Artificial plant biofilms could be scraped
157 directly with a sterile scalpel.

158 *2.4 Analysis methods*

159 *2.4.1 Extracting and purifying of samples* (Hussain et al., 2016; Zhao et al., 2014)

160 Sediment samples: 5.0 g of lyophilization sediment samples and 2.0 g anhydrous
161 sodium sulfates were mixed and soaked in 15 mL extractant agent (hexane / acetone =
162 2/1, v/v) for 1 h in 50 mL glass centrifuge tube, and processed 10 min ultrasonic extraction.
163 The above-mentioned process was repeated twice, and the supernatants were moved to
164 the pear-shaped bottle and concentrated to 1 mL with vacuum rotary evaporator for
165 purifying. After the Solid Phase Purification Column (SPPC, 0.5 g copper powder + 1 g
166 anhydrous sodium sulfate + 1g silica gel + 1 g alumina pretreated) was rinsed and
167 activated with 5 mL *n*-hexane, the concentrated extracting liquor was transferred to the
168 SPPC and eluted by 15 mL *n*-hexane and 10 mL dichloromethane. The obtained eluent
169 was concentrated and adjusted to 1 mL with *n*-hexane.

170 Water samples (Zhao et al., 2018): After each water sample (1 L) was filtrated through
171 glass fiber membrane of 0.45 μm and extracted with C18 SPE column, the column was

172 washed by HPLC water, and pumped for 30 minutes to remove redundant moisture. The
173 PAHs in the SPE column was eluted with 10 mL of acetone/*n*-hexane ($v/v=1/2$) and 12
174 mL of dichloromethane/*n*-hexane ($v/v=3/2$). The eluent was concentrated and adjusted to
175 1 mL with *n*-hexane.

176 Plant samples (Tao et al., 2006; Zhao et al., 2018): 5.0 g plant samples and 5.0 g
177 anhydrous sodium sulfates were packed in a filter paper parcel and extracted in Soxhlet
178 Extractor for 10 h with 100 mL 10% of acetone/*n*-hexane (v/v) mixed solvent, and the
179 extracted liquid was washed twice in separating funnel by 5% sodium sulfate solution for
180 removing acetone. The extract of *n*-hexane was concentrated to about 1 mL and dealt with
181 20 mL concentrated sulfuric acid to get rid of the fat in plant samples twice. Finally, the
182 extract was put into SPPC, the purification and elution steps were same as sediments.

183 *2.4.2 Determination of phenanthrene* (Jiao et al., 2007).

184 The phenanthrene was analyzed by Agilent1100 HPLC with fluorescence and UV -
185 adsorption detector. A 250 mm × 4.6 mm × 5 μm reversed phase C18 column (Agilent
186 ZORBAX Eclipse XDB-C18) was used as the stationary phase. A solution of acetonitrile
187 and ultrapure water was delivered as the mobile phase in a gradient programme at 1
188 mL/min. The volume ratio of acetonitrile and water was 75: 25. Phenanthrene was
189 quantified by using external standard solutions sourced from Ehrenstorfer (Augsburg,
190 Germany). Detective wavelength with FLD signals: $Ex\lambda=257$ nm, $Em\lambda=380$ nm.

191 *2.4.3 DNA extraction, PCR amplification, sequencing and data analysis*

192 Weighing 0.5 g biofilm-leaves/-surface samples in 2 mL centrifuge tube, the bacterial

193 DNA were extracted by Soil DNA Kit (Omega E.Z.N.A.TM, Omega Bio-Tech) according
194 to manufacturer's protocol. The PCR primers were V3-V4 universal primers 341F/805R
195 (341F: CCTACGGGNGGCWGCAG; 805R: GACTACHVGGGTATCTAATCC)
196 provided by Sangon Biotech Co., Ltd., Shanghai, China. The PCR reaction mixture
197 contained 5 μ L 10 \times PCR buffer, 0.5 μ L dNTPs (10 mM each), 0.5 μ L Bar-PCR primer F
198 (50 μ M), 0.5 μ L Primer R (50 μ M), 0.5 μ L Plantium Taq (5 U/ μ L), 10 ng DNA template,
199 with sterile water added to make the final volume to 50 μ L. The following PCR cycle was
200 performed: initial denaturation at 94 $^{\circ}$ C for 3 min, denaturation at 94 $^{\circ}$ C for 30 s,
201 renaturation at 94 $^{\circ}$ C for 30 s, annealing at 45 $^{\circ}$ C for 20 s, extension at 65 $^{\circ}$ C for 30 s with
202 a total of 30 cycles, and the final extension at 72 $^{\circ}$ C for 5 min. Amplification products
203 were detected by 1% agarose gel electrophoresis, and then recycled using DNA Recycle
204 Kit, SK8131 (Sangon Biotech Co., Ltd, Shanghai, China), and finally quantified using
205 Qubit 2.0 DNA Assay Kit (Sangon Biotech Co., Ltd, Shanghai, China). Paired-end
206 sequencing was performed using Illumina MiSeq platform (Illumina, San Diego, CA,
207 USA).

208 Sequencing analysis was executed by using QIIME (Yu et al., 2017). The Uclust
209 method was used to pick the representative sequences for each operational taxonomic
210 units (OTUs). Then the taxonomic information was annotated with the SILVA database
211 after subsampling based on the lowest number of reads. The number of reads ranged from
212 35410 to 46153. Alpha diversity refers to the diversity of microorganism in a special
213 region or ecosystem. A number of Alpha diversity measures were evaluated using the

214 Mothur software including the abundance based coverage estimator (ACE), terminal
215 richness estimation (Chao1), the Shannon index, Simpson index and the Good's coverage
216 estimation. Statistical analyses were performed using R software, including rank-
217 abundance curves, microbial community composition at phylum and genus level, PCoA
218 and hierarchical cluster analysis using Bray-Curtis algorithm. Among them, PCoA and
219 hierarchical cluster analysis were usually used to research the similarity or difference of
220 microbial community composition of different samples group. Heat maps generated by
221 HemI can reflect visually the difference in abundance distribution of species between
222 different groups. The difference of microbial communities at genus level was analyzed
223 by Kruskal-wallis H test and Wilcoxon rank-sum test using STAMP software, which is
224 used to assess the difference of Alpha diversity indices based on three classifications. In
225 addition, one-way ANOVA was applied to check the difference of ECI between four
226 systems.

227 The raw DNA sequence data was uploaded to NCBI Short Read Archive (SRA) with
228 the accession number of SRP125077.

229 **3. Results and discussion**

230 *3.1 Phenanthrene dissipation and ecological contribution of submerged macrophytes and*
231 *their biofilm-leaves*

232 *3.1.1 Dissipation of phenanthrene in water, sediment and leaves*

233 During the experiment, phenanthrene concentration in sediments declined with the
234 time in all the treatments (Fig. 1a). The dissipated efficiencies were in the order of VN

235 (62.7% for 20 mg/kg and 64.1% for 10 mg/kg) > HV (51.1% and 58.4%) \cong AP (51.6%
236 and 53.5%) > CG (35.8% and 42.4%). The results indicated that submerged macrophytes
237 settled in sediments could contribute to the removal of phenanthrene, with dissipation
238 rates dependent on the type of submerged macrophytes. This may relate to the capabilities
239 of oxygenation and microbiological degradation of root tissue (He and Chi, 2016) and the
240 biofilm-leaves.

241 The phenanthrene concentrations in water were rather low because of its
242 hydrophobicity and low solubility (Fig. 1b); most phenanthrene was adsorbed in
243 sediments (Fig. 1a) or on the surface of submerged macrophytes (Fig. 1c). The
244 phenanthrene concentrations in water showed an initial increase followed by a gradual
245 decrease slowly (Fig. 1b), while the phenanthrene concentrations in leaves always kept a
246 relatively stable level in two kinds of hydrophyte leaves and were approximately 200
247 times greater than in water (Fig. 1b, Fig. 1c). The concentrations of phenanthrene in leaves
248 were lower by an order of magnitude than in sediments (Fig. 1a, Fig. 1c), due to the
249 mutual exchange balance of PAHs among overlying water, leaves and sediment (Diepens
250 et al., 2014) and low level of phenanthrene in water naturally.

251 *3.1.2 Ecological contribution of submerged macrophytes and their biofilm-leaves*

252 Actually, the dissipation mechanisms of phenanthrene in different treatments system
253 are very complicated and include many dissipated processes, which may contain
254 synergies and antagonisms and be difficult to identify the sole dissipated contribution. In
255 order to understand the combined dissipation ecological contribution of different

256 treatments (e.g. background dissipation, volatilization, photolysis) well, we regarded the
257 dissipation of phenanthrene as the sum of dissipated contribution of different dissipation
258 mechanism and ignored the synergies and antagonisms among them probably.
259 Considering the giant area of leaves and its ability of releasing oxygen of submerged
260 macrophytes at the same time, we should give weight to the contribution of biofilm-leaves
261 in remediating PAHs polluted sediments. So, we set an ecological contribution index (ECI)
262 to evaluate the contribution of each system in remediating Phe-polluted sediments (Fig.
263 1d).

$$264 \quad \text{ECI} = (\text{spiked conc.} - \text{residual conc.}) * 100 / \text{spiked conc.} \% \quad (1)$$

265 ECI was in order of VN (36.8%-62.7%) > HV (30.2%-51.10%) > AP (27.6%-51.6%) >
266 CG (7.1%-35.8%) in 20 mg/kg phenanthrene system, and VN (40.3%-64.1%) > HV
267 (33.2%-58.4%) > AP (30.3%-53.5%) > CG (14.6%-42.4%) in 10 mg/kg phenanthrene
268 system from 14 d to 35 d, respectively. One-way ANOVA followed by DUNCAN post
269 hoc test was performed to check the difference of ECI among these four systems. And
270 results showed that there were no significant difference appeared regarding the PAHs
271 concentration ($p=0.078$ for 20 mg/kg; $p=0.233$ for 10 mg/kg); however, the ECI of
272 VN/HV system, especially for VN system was higher than AP/CG system spiked by 20
273 mg/kg phenanthrene rather than 10 mg/kg phenanthrene. Actually, the dissipation of
274 phenanthrene in CG system comes from the background dissipating ability, which
275 includes the volatilization, photolysis, release from sediment to water, microbiological
276 degradation in water and sediment. The dissipation of phenanthrene in AP system comes

277 from the background dissipating ability and the adsorption of artificial plant and the
278 degradation by the biofilm attached on the artificial plant surface. In the submerged
279 macrophytes system, phenanthrene dissipation can be explained by the action of
280 rhizosphere microbes, in addition to the factors acting in the AP. The difference of
281 dissipation between the AP and CG systems can represent the ecological contribution of
282 artificial plant biofilm (15.0%-20.5% for 20 mg/kg phenanthrene and 11.1%-15.6% for
283 10 mg/kg phenanthrene, and the averages were 17.1% and 13.2%, respectively), and the
284 ecological contribution of rhizosphere microbes can be represented by the difference of
285 dissipation between submerged macrophytes system and AP system (9.2%-11.7% in 20
286 mg/kg phenanthrene and 9.1%-10.6% in 10 mg/kg phenanthrene system for VN, the
287 average was 9.9%-10.6%; and 0%-5.4% in 20 mg/kg phenanthrene system and 1.6%-4.9%
288 in 10 mg/kg phenanthrene system for HV, the average was 2.5%-3.2%).

289 Our research confirmed phenanthrene released from sediments to water then
290 accumulated on the leaves surface of submerged macrophytes. We also noticed the
291 dissipation of phenanthrene in water and sediments during the cultivation process (Fig.
292 1a and Fig. 1b). It may be related to the dissipation induced by physical and chemical
293 process (e.g. photodecomposition), the enrichment and dissipation of hydrophyte (Li et
294 al., 2009), and the degradation of microorganisms. In addition, the added organic matters
295 could improve the adsorption capacity of sediment on phenanthrene because the dead
296 leaves sank into sediments later (Ying-Heng et al., 2014). However, the steady
297 phenanthrene concentration in the leaves of submerged macrophytes might be related to

298 the length of incubation time (Liu et al., 2014).

299

300

Figure 1

301

302 *3.2 Bacterial diversity analysis based on attached surface, spiking concentration and*

303 *incubation time*

304 *3.2.1 Alpha diversity*

305 Alpha diversity can show the diversity of microorganism in a special region or

306 ecosystem. In this study, the alpha diversities of biofilm microbial indices for leaf surface

307 were shown in Table 1. ACE and Chao 1 are designed to estimate the community richness

308 of biofilm samples based on the OTU numbers. The values of ACE and Chao 1 showed

309 that the community richness of microbes in artificial plant samples (1C and 2C) were far

310 higher than those submerged plant samples (1A, 2A, 3A, 4A and 1B, 2B, 3B, 4B), and

311 the community richness of VN were slightly higher than those of HV. The Shannon and

312 Simpson indices reflect community diversity. In our present study, the community

313 diversity was consistent with community richness. The incubation time significantly

314 affected the community diversity of biofilm samples, and those of 14 d samples were

315 higher than those of 28 d samples. However, the effect of phenanthrene concentration was

316 indistinctive. The coverage index represents the sequencing depth. In the study, the

317 coverage was approximately equal to 0.99 except for 1C (0.97) and 2C (0.97) after

318 subsampling based on the lowest number of reads, and indicating all the samples reflected

319 the actual situation. Meanwhile, the difference was analyzed among Alpha indices based
320 on three classifications (attached surface, spiking concentration of phenanthrene and
321 incubation time) using Wilcoxon rank-sum test (Table S1). However, there was not
322 statistically significant difference regretfully ($p < 0.05$, see the Table S1).

323

324

Table 1

325

326 *3.2.2 Taxon richness and distribution evenness analysis: Rank-abundance distribution*
327 *curves, Shannon-Wiener curves and Rarefaction curves of the OTUs*

328 Applying the rank-abundance curve to analyze species distribution was an imperative
329 manner. On account of computing the sequencing numbers which each OTU contained,
330 researchers sorted by OTUs in descending order and depicted the relevant relations in
331 accordance with abundance. The curves can reflect both species abundance and
332 distribution evenness (Cheng et al., 2016). Fig. 2 showed that the distribution ranges of
333 AP were wider than SM, which demonstrated that the species in the biofilm-surface of
334 AP were more abundant. The curve graph of SM was smaller than that of AP, which meant
335 that the species distribution was more even in AP. The rank-abundance distribution
336 corresponded to the analysis of community diversity using Alpha diversity indices.

337 The Shannon-Wiener curves takes richness and evenness of samples into account.
338 Sample 10B had the highest diversity (6.64) and followed by sample 9B (6.53), while the
339 sample 3B had the lowest diversity (4.00) (Fig S1a). The reads of each sample were large

340 enough (>25,000 tags per sample) to reflect huge diversity of microbial community
341 because they reached the plateau since less than 5,000 tags for each sample. Rarefaction
342 analysis was applied to standardize and compare taxon richness observed among samples
343 (Fig. S1b). The rarefaction curves based on OTUs (97% similarity) presented a generally
344 consistent tendency for SM rather than AP. These results showed that recovered
345 sequences reflected the diversity of microbial community well, and further sampling
346 could reveal the diversity of microbial community in AP to some extent.

347 *3.2.3 Beta diversity*

348 The Beta diversity is good at comparing the microbial community composition among
349 different sample groups. Here, it was assessed by PCoA based on OTU level, and the
350 results were illustrated in Fig. 3a. Principal components 1 (PC1) and PC2 explained 42.5%
351 and 18.79% of variation of microbial community composition, respectively. Generally,
352 the samples were divided into three groups (group A, group B and group C). The different
353 attached surface (AP: group C vs. SM: group A and group B) had a dominant influence
354 on the microbial community structure, but the difference among submerged macrophytes
355 was small. The separation of group A and group B indicated that incubation time also
356 influenced the bacterial community composition. However, the spiking concentration of
357 phenanthrene just presented marked effect on the community structure in VN only.

358 **Figure 2**

359

360 *3.3 Comparison and difference analysis based on attached surface, spiking concentration*

361 *and incubation time at genus level*

362 The bacterial community structures of AP and SM samples at phylum level are shown
363 in Fig. S3. The results reflected that the diversity and evenness of bacterial community
364 on the surface of artificial plant were higher than those on the leaves of submerged
365 macrophytes again. In order to identify and understand the key impact factors (e.g.
366 submerged plants, spiking concentration of and incubation time) on the microorganism
367 composition of biofilm-leaves, Hierarchical clustering analysis, heat map, Kruskal-wallis
368 H test and Wilcoxon rank-sum test were used to analysis and visually show the difference
369 significant of different impact factors.

370 *3.3.1 Hierarchical clustering analysis*

371 Hierarchical clustering dendrograms were usually used to research the similarity or
372 difference of microbial community composition of different samples. And in our study,
373 they were generated at genus level based on attached surface, spiking concentration and
374 incubation time, respectively. From Fig. 3b, all the samples were separated into two
375 distinct groups: AP and SM. And compared to HV, VN had a stronger influence on
376 bacterial community composition at genus level except for sample 1A. While different
377 spiking concentration of phenanthrene had a weak impact on the bacterial community
378 structures at genus level (Fig. 3c). Moreover, bacterial community structures changed
379 along with incubation time at genus level except for 3A (Fig. 3d). These results were
380 consistent with PCoA.

381 *3.3.2 Visual display of difference: Heat maps of bacterial communities*

382 Attached surface, spiking concentration of phenanthrene and incubation time affected
383 bacterial community in one way or another. Heat maps of bacterial communities in top
384 50 genera based on attached surface, spiking concentration and incubation time were
385 drawn to highlight distinctly different specific genera (Fig. 5). Fig. 5a showed that 8
386 genera were abundant in the bacterial community of samples AP, but were rarely
387 identified and appeared in samples SM, including *Pseudomonas*,
388 *norank_c__Acidobacteria*, *norank_f__Anaerolineaceae*, RB1, *Geobacter*, *Nitrospira*,
389 *unclassified_f__Micrococcaceae* and *Sphingomonas*. Previous studies showed that
390 *Pseudomonas* and *Sphingomonas* were PAH-degrading bacteria, and *nitrospira sp.* was
391 associated with nitrogen cycling. *Norank_c__Cyanobacteria*,
392 *unclassified_f__Comamonadaceae* and *Pirellua* were abundant in samples SM. A few
393 genera were abundant in samples VN, such as *unclassified_c__Cyanobacteria*,
394 *Limnothrix* and *unclassified_f__FamilyI_o__SubsectionI*.

395 Fig. 5b presented *unclassified_f__FamilyI_o__SubsectionI*, *unclassified_f__*
396 *Comamonadaceae*, *unclassified_c__Cyanobacteria*, *Limnothrix* and *Pseudorhodofera*
397 were observed to be abundant in the lower concentration groups (10 mg/kg), while only
398 one genus, *norank_c__Cyanobacteria*, was found in abundance among the higher
399 concentration groups (20 mg/kg).

400 Only two genera, *Limnothrix* and *Ideonella*, were detected to be abundant in 14 d (Fig.
401 5c), while *unclassified_c__Cyanobacteria*, *Pesudorhodofera*, *norank_f__FamilyI*,
402 *unclassified_f__FamilyI_o__SubsectionI* and *norank_o__Caenarcaniphilales* were

403 abundant in 28 d.

404 **Figure 3**

405

406 *3.3.3 Difference significance level analysis: Kruskal-wallis H test and Wilcoxon rank-*
407 *sum test*

408 In order to assess the significance level of abundance difference of species and obtain
409 the significantly different species, Kruskal-wallis H test and Wilcoxon rank-sum test were
410 used to identify the difference between the top 60 genera based on attached surface (Fig.
411 6a), and top 15 genera based on spiking concentration of phenanthrene (Fig. 6b) and
412 incubation time (Fig. 6c), respectively. Only five genera including
413 *norank_c__Cyanobacteria* ($p=0.04227$), *Limnothrix* ($p=0.04973$), *norank_f__MNG7*
414 ($p=0.0197$), *norank_f__Gemmatimonadaceae* ($p=0.0379$) and
415 *unclassified_f__FamilyI_o__SubsectionIII* ($p=0.01927$) presented a significant
416 difference from top 40 genera in Fig. 4a. We observed that *norank_c__Cyanobacteria*,
417 *Limnothrix* and *unclassified_f__FamilyI_o__SubsectionIII* belonged to the phylum of
418 Cyanobacteria, *norank_f__MNG7* belonged to the phylum of Proteobacteria, and
419 *norank_f__Gemmatimonadaceae* belonged to the phylum of Gemmatimonadetes.
420 However, there were 9 genera presented significant difference from the last 15 rare genera
421 in top 60 genera. There was no significant difference between the top 15 genera (Fig 4b).
422 Seen in Fig. 4c, four genera in top 15 genera presented significant difference consisting
423 of *Ideonella* ($p=0.03038$), *Bryobacter* ($p=0.03038$), *Gemmata* ($p=0.03038$) and

424 *Planctomyces* ($p=0.03038$). *Ideonella* belonged to the phylum of Proteobacteria,
425 *Gemmata* and *Planctomyces* belonged to the phylum of Planctomycetes. These results
426 indicated that attached surface dominating in bacterial community tended to influence the
427 genera with lower relative abundance more than incubation time, while spiking
428 concentration of phenanthrene did not tend to affect the genera significantly.

429

430

Figure 4

431

432 *3.4 The influence mechanism of attached surface, spiking concentration and incubation*
433 *time on microbial community*

434 In our present study, SM had a more important role in biofilm establishment than AP.
435 This was most likely related to allelochemicals secreted by submerged macrophytes (e.g.
436 phenolic acids, fatty acids, alkaloids, terpenes and flavonoids) (Weston and Mathesius,
437 2013; Zi et al., 2014), which could restrict the growth of algae, cyanobacteria and
438 heterotrophic bacteria, and affected biofilm composition. In addition, submerged
439 macrophytes not only secreted organic substances to provide carbon source for the
440 microorganisms of the biofilm, but also released oxygen by photosynthesis, which leded
441 to the change of micro-interfaces environment (e.g. DO, ORP and pH) day and night.
442 These activities also influenced the composition of bacterial communities attached on
443 leaves of submerged plants (Hempel et al., 2009). Of course, the morphological and
444 physiological complexity of submerged macrophytes could provide a diversity of

445 microhabitats for organisms to live in (Goldsborough et al., 2005). Several researchers
446 had insisted that periphyton communities correlated with macrophytes were highly host-
447 specific (Kahlert and Pettersson, 2002; Wetzel, 1983).

448 The bacterial community was not obviously affected by the phenanthrene spiked in
449 surficial sediments in different concentrations. This might be related to the lower
450 concentration and smaller concentration gradient of phenanthrene on the leaves surface
451 by different migration routine (Fig. 1c). Phenanthrene can transfer in the macrophytes
452 tissues from root to leaves after it is absorbed from sediment; however, this may not be a
453 reliable pathway as phenanthrene translocation from roots to shoots can be limited (Liu
454 et al., 2014), let alone to leaves. An alternative explanation is that phenanthrene is released
455 from sediments into water and then to leaves. Recent studies suggested that phenanthrene
456 could be dissipated by rhizospheric microorganisms or fixed by sediments (He and Chi,
457 2016; He et al., 2016; Liu et al., 2014), and small amounts of phenanthrene were released
458 from sediments due to low solubility in water (1.18 mg/L). In addition, leaves of
459 submerged macrophytes could absorb from or release to overlying water for phenanthrene
460 (Diepens et al., 2014). Thus the contents of phenanthrene accumulated in leaves of
461 submerged macrophytes were rather limited (Fig. 1c and Fig. 1d), making it difficult to
462 change the composition of biofilm. If phenanthrene was directly accumulated by leaves
463 from water, results would be other cases which needed our future study.

464 Incubation time had a marked effect on the bacterial community of biofilm attached on
465 leaves of submerged macrophytes. We attributed this phenomenon to the growth status of

466 biofilm possibly (Cai et al., 2013). Several researches suggested that epiphytic microbes
467 were difficult to attach on the healthy leaves (Jennings and Steinberg, 1997; Peterson et
468 al., 2007). And the self-destruction of aged leaves produced plenty of dissolved
469 substances to facilitate the development of epiphytic microbes. Meanwhile, the
470 phenanthrene accumulated in leaves of submerged macrophytes was stable from 14 d to
471 35 d. We did not find out the PAH-degrading bacteria presented significant difference
472 (Fig. 6c), which might be related to the reality that these bacteria did not occupy the
473 dominating positions in nature. In our future study, we will put more emphasis on the
474 ascertaining response of the functional bacteria in the biofilm attached on leaves of
475 submerged macrophytes to organic and high-toxic pollutants like PAHs.

476 **4. Conclusions**

477 Our study suggested that biofilm-leaves could contribute to remediation of sediment
478 polluted by phenanthrene. Attached surface had an important effect on bacterial
479 community composition of biofilm-leaves/-surface due to the active interface influence
480 of submerged macrophytes. Incubation time changed the bacterial community, which
481 might explain differences in growth and mature state of the biofilm. Phenanthrene spiking
482 concentration in sediment did not appear to markedly influence bacterial community –
483 which may be due to the lower concentration and smaller concentration gradient of
484 phenanthrene on the leaf surfaces. On the whole, phenanthrene concentration spiked in
485 sediment, aquatic plant categories and incubation time affected the bacterial community
486 on biofilm-leaves with varying degrees.

487 **Acknowledgements**

488 This work was supported by the National Natural Science Foundation of China (Grants
489 No. 51879080, 51509129 and 41371307), Natural Science Foundation of Jiangsu
490 Province, China (BK20171435), National Key Research & Development Program of
491 China (No. 2018YFC0407906), the Open Foundation of State Key Laboratory of
492 Pollution Control and Resource Reuse (Grant No. PCRRF12010), the State Key
493 Laboratory of Soil and Sustainable Agriculture (Institute of Soil Science, Chinese
494 Academy of Sciences) foundation (Grant No. 0812201228), a project funded by the
495 Priority Academic Program Development of Jiangsu Higher Education Institutions
496 (PAPD), and the Top-notch Academic Programs Project (TAPP) of Jiangsu Higher
497 Education Institutions.

498 **References**

499 Agarwal, S., Al-Abed, S.R., Dionysiou, D.D., 2007. In Situ Technologies for
500 Reclamation of PCB-Contaminated Sediments: Current Challenges and Research Thrust
501 Areas. *Journal of Environmental Engineering* 133, 1075-1078.

502 Bamforth, S.M., Singleton, I., 2010. Bioremediation of polycyclic aromatic
503 hydrocarbons: current knowledge and future directions. *Journal of Chemical*
504 *Technology & Biotechnology* 80, 723-736.

505 Cai, X., Gao, G., Tang, X., Dong, B., Dai, J., Chen, D., Song, Y., 2013. The response of
506 epiphytic microbes to habitat and growth status of *Potamogeton malaianus* Miq. in Lake
507 Taihu. *Journal of Basic Microbiology* 53, 828–837.

508 Cheema, S.A., Imran, K.M., Shen, C., Tang, X., Farooq, M., Chen, L., Zhang, C., Chen,

509 Y., 2010. Degradation of phenanthrene and pyrene in spiked soils by single and
510 combined plants cultivation. *Journal of Hazardous Materials* 177, 384-389.

511 Chen, M., Xu, P., Zeng, G., Yang, C., Huang, D., Zhang, J., 2015. Bioremediation of
512 soils contaminated with polycyclic aromatic hydrocarbons, petroleum, pesticides,
513 chlorophenols and heavy metals by composting: Applications, microbes and future
514 research needs. *Biotechnology Advances* 33, 745.

515 Cheng, Z., Hu, X., Sun, Z., 2016. Microbial community distribution and dominant
516 bacterial species analysis in the bio-electrochemical system treating low concentration
517 cefuroxime. *Chemical Engineering Journal* 303, 137-144.

518 Diepens, N.J., Arts, G.H., Focks, A., Koelmans, A.A., 2014. Uptake, translocation, and
519 elimination in sediment-rooted macrophytes: a model-supported analysis of whole
520 sediment test data. *Environmental Science & Technology* 48, 12344.

521 Goldsborough, L.G., Mcdougal, R.L., North, A.K., Azim, M.E., Verdegem, M.C.J., Van
522 Dam, A.A., Beveridge, M.C.M., 2005. Periphyton in freshwater lakes and wetlands.

523 Gomes, H.I., Dias-Ferreira, C., Ribeiro, A.B., 2013. Overview of in situ and ex situ
524 remediation technologies for PCB-contaminated soils and sediments and obstacles for
525 full-scale application. *Science of the Total Environment* 445-446, 237.

526 Hassan, H.M., Castillo, A.B., Yigiterhan, O., Elobaid, E.A., Al-Obaidly, A., Al-Ansari,
527 E., Obbard, J.P., 2018. Baseline concentrations and distributions of Polycyclic Aromatic
528 Hydrocarbons in surface sediments from the Qatar marine environment. *Marine
529 Pollution Bulletin* 126, 58.

530 He, D., Ren, L., Wu, Q., 2012. Epiphytic bacterial communities on two common
531 submerged macrophytes in Taihu Lake: diversity and host-specificity. Chinese journal
532 of oceanology and limnology 30, 237-247.

533 He, Y., Chi, J., 2016. Phytoremediation of sediments polluted with phenanthrene and
534 pyrene by four submerged aquatic plants. Journal of Soils & Sediments Protection Risk
535 Assessment & Rem 16, 309-317.

536 He, Y., Chi, J., Qi, Y., 2016. Response of bacterial community structure to
537 disappearance of phenanthrene and pyrene from sediment with different submerged
538 macrophytes. Ecological Engineering 91, 207-211.

539 Hempel, M., Grossart, H.P., Gross, E.M., 2009. Community composition of bacterial
540 biofilms on two submerged macrophytes and an artificial substrate in a pre-alpine lake.
541 Aquatic Microbial Ecology 58, 79-94.

542 Hussain, J., Zhao, Z., Pang, Y., Xia, L., Hussain, I., Jiang, X., 2016. Effects of Different
543 Water Seasons on the Residual Characteristics and Ecological Risk of Polycyclic
544 Aromatic Hydrocarbons in Sediments from Changdang Lake, China. Journal of
545 Chemistry,2016,(2016-2-11) 2016.

546 Jérôme Cachot, †, Mac Law, Didier Pottier, Laurent Peluhet, Michelle Norris, H el ene
547 Budzinski, A., Richard Winn, 2007. Characterization of Toxic Effects of Sediment-
548 Associated Organic Pollutants Using the λ Transgenic Medaka. Environmental Science
549 & Technology 41, 7830-7836.

550 Jennings, J.G., Steinberg, P.D., 1997. Phlorotannins versus Other Factors Affecting

551 Epiphyte Abundance on the Kelp *Ecklonia radiata*. *Oecologia* 109, 461-473.

552 Jiao, X.C., Xu, F.L., Dawson, R., Chen, S.H., Tao, S., 2007. Adsorption and absorption
553 of polycyclic aromatic hydrocarbons to rice roots. *Environmental Pollution* 148, 230-
554 235.

555 Jones, J.I., Eaton, J.W., Hardwick, K., 2000. The influence of periphyton on boundary
556 layer conditions: a pH microelectrode investigation. *Aquatic Botany* 67, 191-206.

557 Kahlert, M., Pettersson, K., 2002. The impact of substrate and lake trophic on the
558 biomass and nutrient status of benthic algae. *Hydrobiologia* 489, 161-169.

559 Kim, H.B., Isaacson, R.E., 2015. The pig gut microbial diversity: Understanding the pig
560 gut microbial ecology through the next generation high throughput sequencing.
561 *Veterinary Microbiology* 177, 242-251.

562 Li, H., Qu, R., Li, C., Guo, W., Han, X., He, F., Ma, Y., Xing, B., 2014. Selective
563 removal of polycyclic aromatic hydrocarbons (PAHs) from soil washing effluents using
564 biochars produced at different pyrolytic temperatures. *Bioresour Technol* 163, 193-198.

565 Li, J.H., Guo, H.Y., Wang, X.R., Minghong, W., Wang, S.H., Yin, D.Q., Yin, Y., Zhang,
566 J.F., Munawar, M., 2009. Plant-promoted dissipation of four submerged macrophytes to
567 phenanthrene. *Aquatic Ecosystem Health & Management* 12, 471-476.

568 Liang, Y., Tse, M.F., Young, L., Wong, M.H., 2007. Distribution patterns of polycyclic
569 aromatic hydrocarbons (PAHs) in the sediments and fish at Mai Po Marshes Nature
570 Reserve, Hong Kong. *Water Research* 41, 1303.

571 Lin, Y., Deng, W., Li, S., Li, J., Wang, G., Zhang, D., Li, X., 2016. Congener profiles,

572 distribution, sources and ecological risk of parent and alkyl-PAHs in surface sediments
573 of Southern Yellow Sea, China. *Science of the Total Environment* 580, 1309-1317.

574 Liu, H., Meng, F., Tong, Y., Chi, J., 2014. Effect of plant density on phytoremediation of
575 polycyclic aromatic hydrocarbons contaminated sediments with *Vallisneria spiralis*.
576 *Ecological Engineering* 73, 380-385.

577 Lu, X.Y., Li, B., Zhang, T., Fang, H.H., 2012. Enhanced anoxic bioremediation of
578 PAHs-contaminated sediment. *Bioresource Technology* 104, 51-58.

579 Ma, B., Yan, H., Chen, H.H., Xu, J.M., Rengel, Z., 2010. Dissipation of polycyclic
580 aromatic hydrocarbons (PAHs) in the rhizosphere: synthesis through meta-analysis.
581 *Environmental Pollution* 158, 855-861.

582 Meng, F., Chi, J., 2016. Effect of *Potamogeton crispus* L. on bioavailability and
583 biodegradation activity of pyrene in aged and unaged sediments. *Journal of Hazardous*
584 *Materials* 324.

585 Meng, F., Huang, J., Liu, H., Chi, J., 2015. Remedial effects of *Potamogeton crispus* L.
586 on PAH-contaminated sediments. *Environmental Science & Pollution Research* 22,
587 7547-7556.

588 Moscoso, F., Tejjiz, I., Deive, F.J., Sanromán, M.A., 2012. Efficient PAHs
589 biodegradation by a bacterial consortium at flask and bioreactor scale. *Bioresource*
590 *Technology* 119, 270-276.

591 Pang, S., Zhang, S., Lv, X.Y., Han, B., Liu, K., Qiu, C., Wang, C., Wang, P., Toland, H.,
592 He, Z., 2016. Characterization of bacterial community in biofilm and sediments of

593 wetlands dominated by aquatic macrophytes. *Ecological Engineering* 97, 242-250.

594 Perelo, L.W., 2010. Review: In situ and bioremediation of organic pollutants in aquatic
595 sediments. *Journal of Hazardous Materials* 177, 81.

596 Peterson, B.J., Frankovich, T.A., Zieman, J.C., 2007. Response of seagrass epiphyte
597 loading to field manipulations of fertilization, gastropod grazing and leaf turnover rates.
598 *Journal of Experimental Marine Biology & Ecology* 349, 61-72.

599 Sandjensen, K., Revsbech, N.P., Jørgensen, B.B., 1985. Microprofiles of oxygen in
600 epiphyte communities on submerged macrophytes. *Marine Biology* 89, 55-62.

601 Srivastava, J.K., Chandra, H., Kalra, S.J.S., Mishra, P., Khan, H., Yadav, P., 2016.
602 Plant–microbe interaction in aquatic system and their role in the management of water
603 quality: a review. *Applied Water Science*, 1-12.

604 Tao, S., Jiao, X.C., Chen, S.H., Liu, W.X., Jr, R.M.C., Zhu, L.Z., Luo, Y.M., 2006.
605 Accumulation and distribution of polycyclic aromatic hydrocarbons in rice (*Oryza*
606 *sativa*). *Environmental Pollution* 140, 406-415.

607 Vila-Costa, M., Pulido, C., Chappuis, E., Calviño, A., Casamayor, E.O., Gacia, E., 2016.
608 Macrophyte landscape modulates lake ecosystem-level nitrogen losses through tightly
609 coupled plant-microbe interactions. *Limnology & Oceanography* 61, 78-88.

610 Wang, L.C., Lee, W.J., Lee, W.S., Changchien, G.P., Tsai, P.J., 2003. Characterizing the
611 emissions of polychlorinated dibenzo-p-dioxins and dibenzofurans from crematories
612 and their impacts to the surrounding environment. *Environmental Science &*
613 *Technology* 37, 62-67.

614 Weston, L.A., Mathesius, U., 2013. Flavonoids: their structure, biosynthesis and role in
615 the rhizosphere, including allelopathy. *Journal of Chemical Ecology* 39, 283-297.

616 Wetzel, R.G., 1983. Attached algal-substrata interactions: fact or myth, and when and
617 how? Springer Netherlands.

618 Yan, L., Zhang, S., Lin, D., Guo, C., Yan, L., Wang, S., He, Z., 2017. Nitrogen loading
619 affects microbes, nitrifiers and denitrifiers attached to submerged macrophyte in
620 constructed wetlands. *Science of the Total Environment* 622-623, 121.

621 Yang, Z., Feng, J., Niu, J., Shen, Z., 2008. Release of polycyclic aromatic hydrocarbons
622 from Yangtze River sediment cores during periods of simulated resuspension.
623 *Environmental Pollution* 155, 366-374.

624 Ying-Heng, F., Baoshan, X., Xiao-Yan, L., 2014. Changes in the adsorption of bisphenol
625 A, 17 α -ethinyl estradiol, and phenanthrene on marine sediment in Hong Kong in
626 relation to the simulated sediment organic matter decomposition. *Environmental*
627 *Pollution* 192, 139.

628 Yu, B., Tian, J., Feng, L., 2017. Remediation of PAH polluted soils using a soil
629 microbial fuel cell: Influence of electrode interval and role of microbial community.
630 *Journal of Hazardous Materials* 336, 110.

631 Zhang, S., Pang, S., Wang, P., Wang, C., Guo, C., Addo, F.G., Li, Y., 2016. Responses of
632 bacterial community structure and denitrifying bacteria in biofilm to submerged
633 macrophytes and nitrate. *Scientific Reports* 6.

634 Zhao, D., Wang, S., Huang, R., Zeng, J., Huang, F., Yu, Z., 2017. Diversity and

635 composition of bacterial community in the rhizosphere sediments of submerged
636 macrophytes revealed by 454 pyrosequencing. *Annals of Microbiology* 67, 313-319.

637 Zhao, Z., Jiang, Y., Xia, L., Mi, T., Yan, W., Gao, Y., Jiang, X., Fawundu, E., Hussain,
638 J., 2014. Application of canonical correspondence analysis to determine the ecological
639 contribution of phytoplankton to PCBs bioaccumulation in Qinhuai River, Nanjing,
640 China. *Environmental Science & Pollution Research International* 21, 3091-3103.

641 Zhao, Z., Xia, L., Jiang, X., Gao, Y., 2018. Effects of water-saving irrigation on the
642 residues and risk of polycyclic aromatic hydrocarbon in paddy field. *Science Of The*
643 *Total Environment* 618, 736-745.

644 Zi, J., Mafu, S., Peters, R.J., 2014. To Gibberellins and Beyond! Surveying the
645 Evolution of (Di)Terpenoid Metabolism. *Annual Review of Plant Biology* 65, 259.

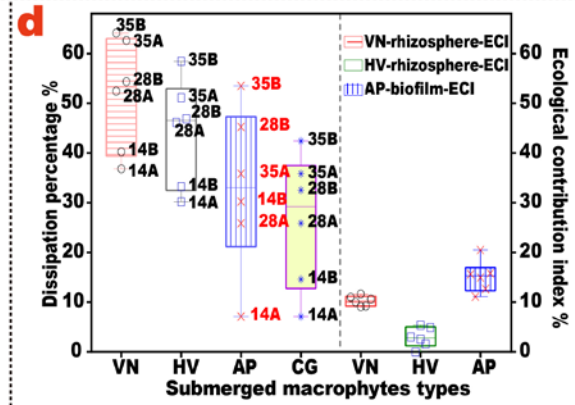
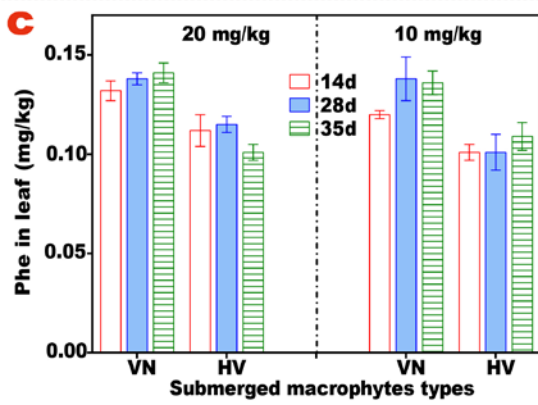
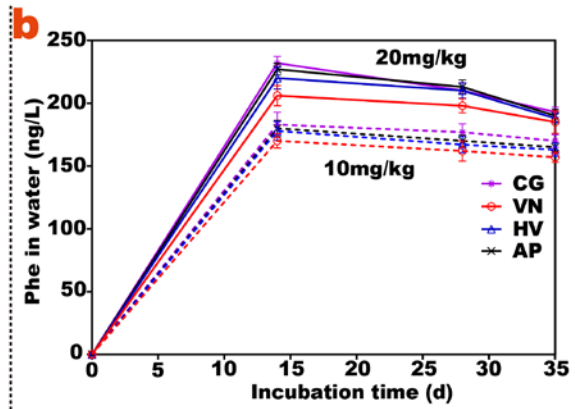
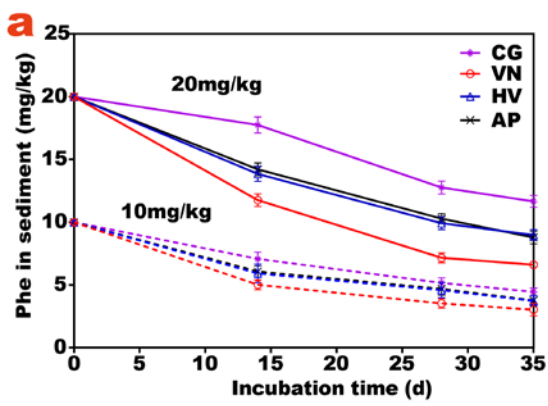
646

647

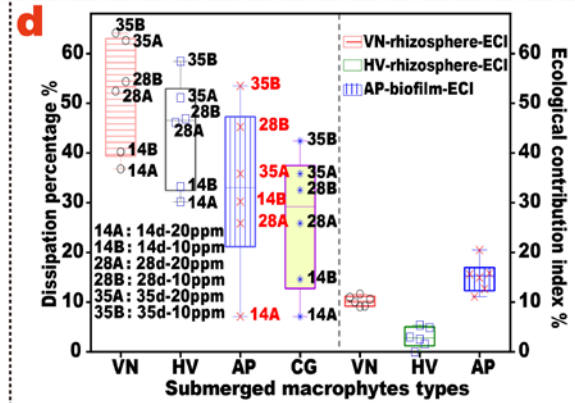
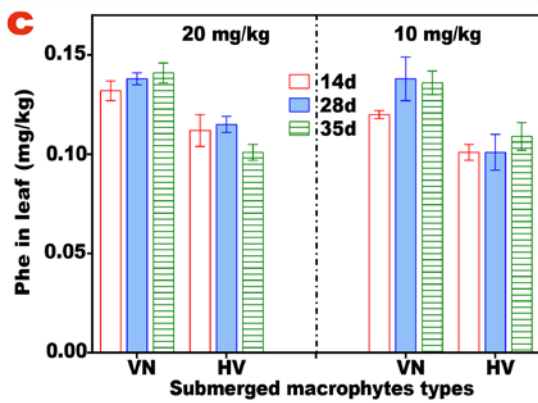
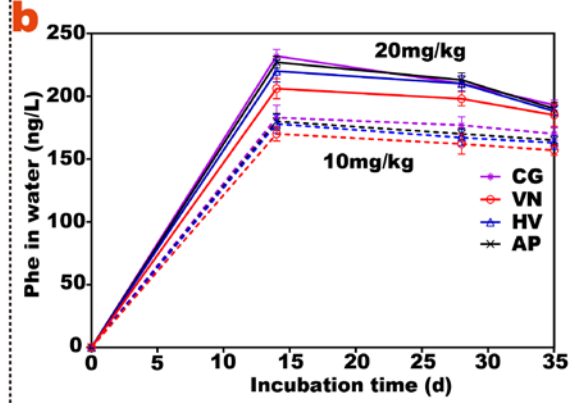
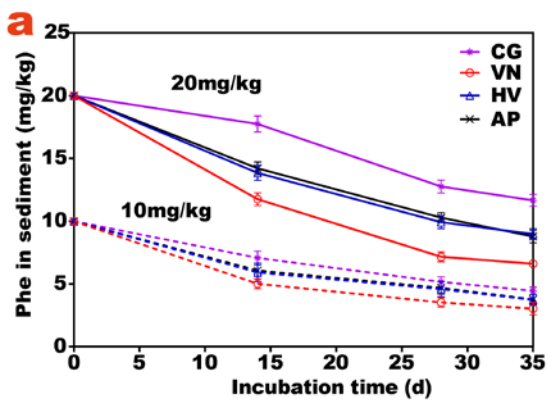
Table 1. Microbial diversity indices in all ten samples

Samples	Phe Conc. mg/kg	Sampling Time	Submerged plants	ACE	Chao 1	Shannon	Simpson	Coverage (%)
1A	20	14d	VN	1535	1526	5.24	0.0156	98.8
2A	20		HV	1561	1593	5.08	0.0254	98.8
3A	10		VN	1551	1617	5.11	0.0240	98.7
4A	10		HV	1591	1621	5.39	0.0129	98.8
1B	20	28d	VN	1568	1590	5.11	0.0236	98.8
2B	20		HV	1451	1550	4.90	0.0407	98.9
3B	10		VN	1894	1694	4.00	0.0761	98.5
4B	10		HV	1262	1265	4.94	0.0213	99.0
1C	20	28d	AP	3916	3823	6.53	0.0053	96.7
2C	10		AP	4070	4036	6.63	0.0061	96.6

649 Note: VN: *Vallisneria natans*; HV: *Hydrilla verticillata*; AP: artificial plants



651

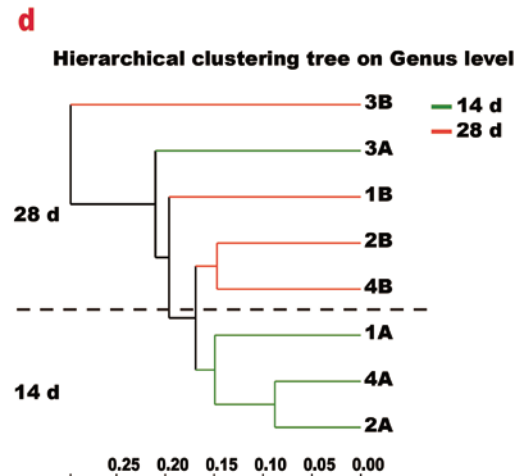
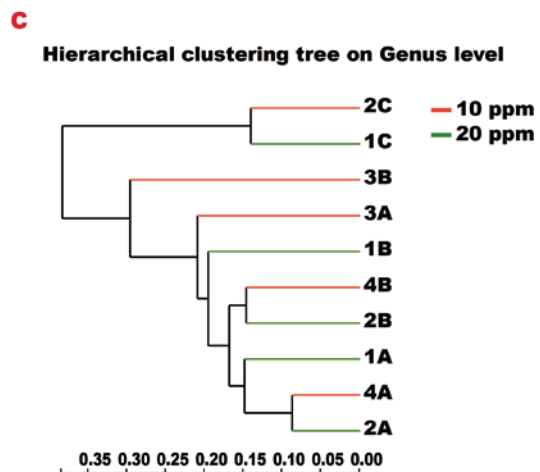
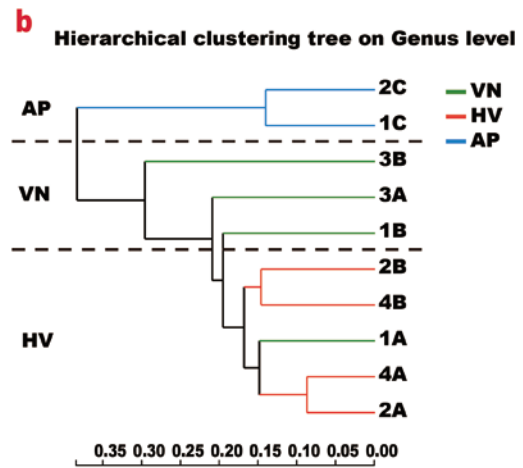
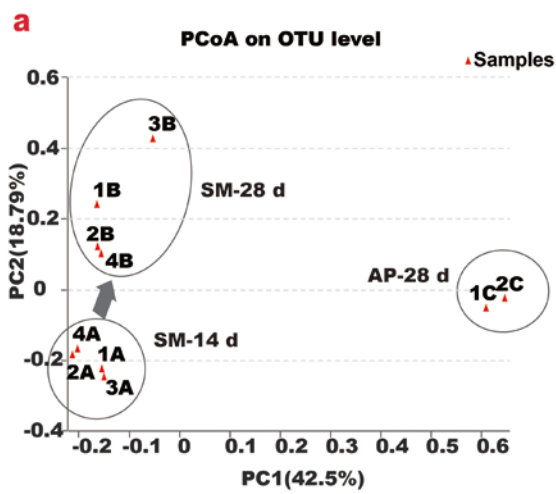


652

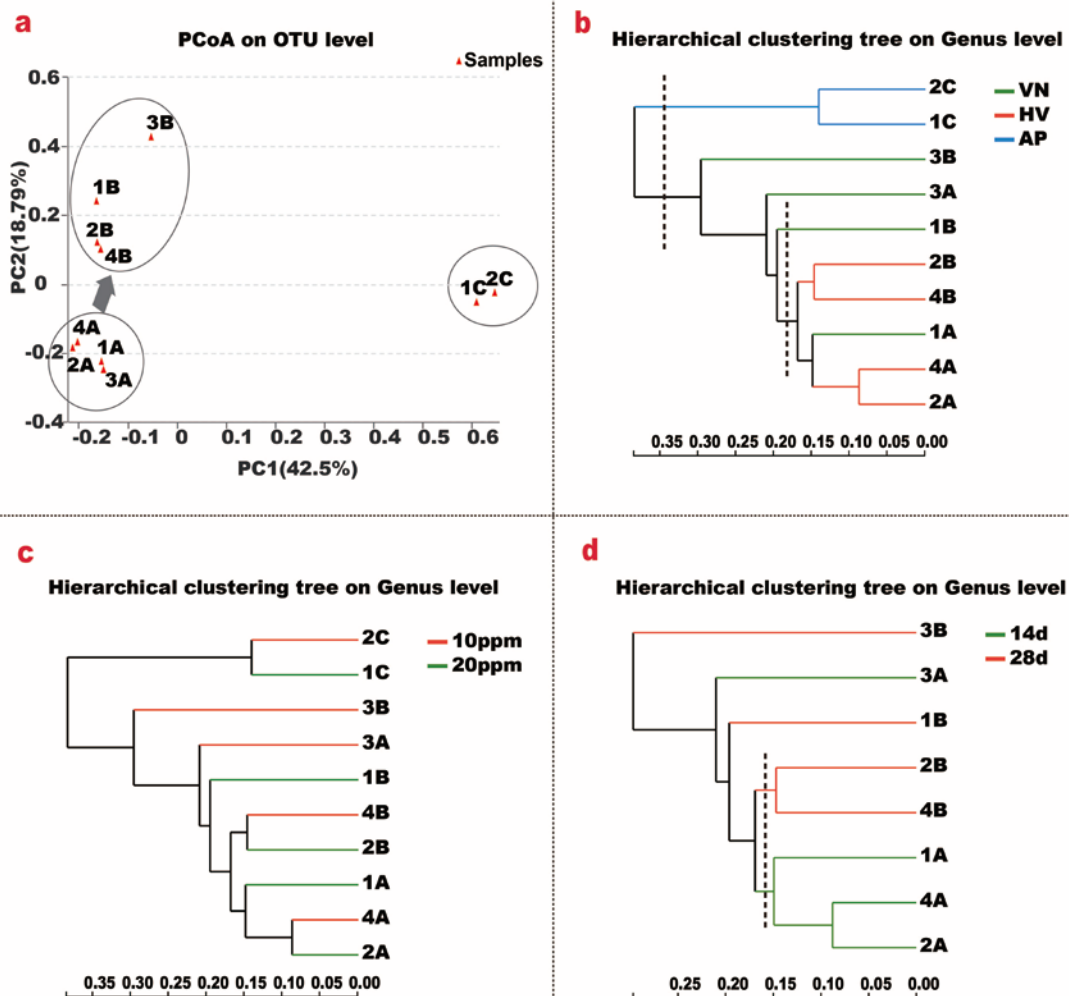
653

654 **Fig. 1.** The residual characteristics of phenanthrene in sediment (**a**), in water (**b**), in leaves
655 of VN and HV (**c**). The dissipation percentage in sediment of VN, HV, AP and CG system,
656 ecological contribution index (ECI) of VN, HV-rhizosphere and AP-biofilm (**d**). The 20
657 mg/kg and 10 mg/kg of phenanthrene concentrations were spiked in sediment initially,
658 respectively. (CG: control group; AP: artificial plant; HV: *Hydrilla verticillata*; VN:
659 *Vallisneria natans*. 14A: 14 d-20 ppm; 14B: 14 d-10 ppm; 28A: 28 d-20 ppm; 28 B: 28
660 d-10 ppm; 35A: 35 d-20 ppm; 35B: 35 d-10 ppm.)

661



662

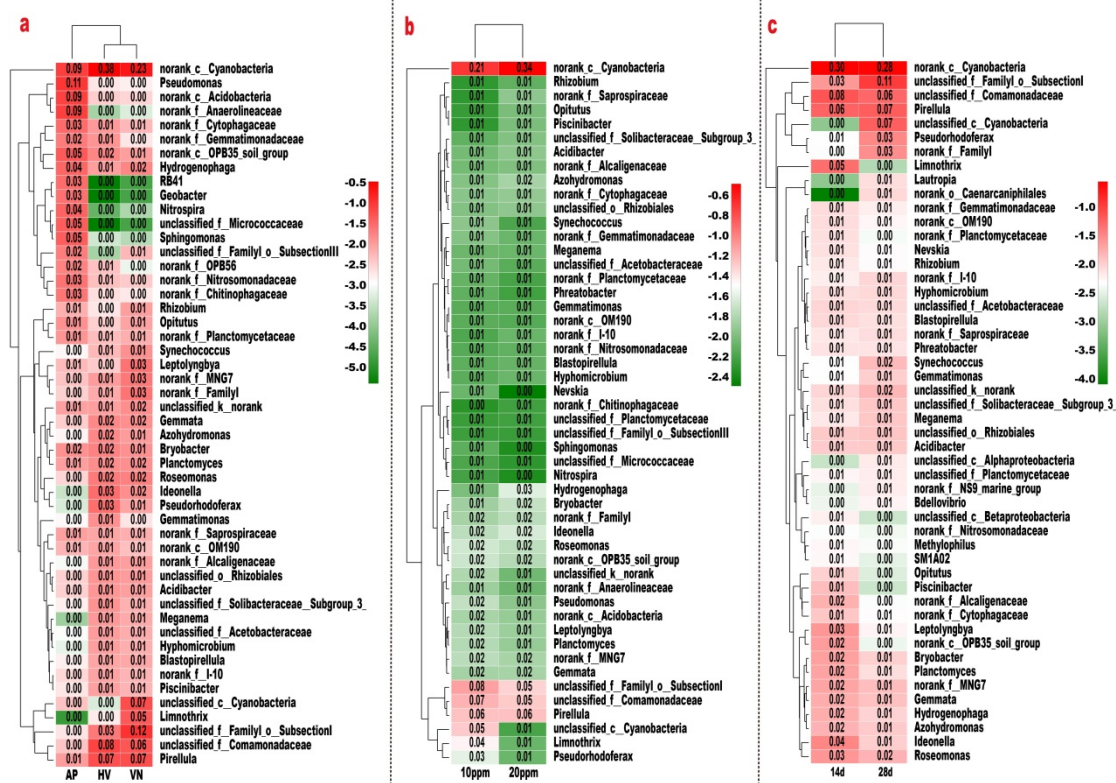


663

664

665 **Fig. 2. a:** Principal coordinates analysis (PCoA) using Bray-Curtis distances for all the
 666 samples on OTU level; **b, c** and **d:** Hierarchical clustering tree using average linkage
 667 between samples at genus level based on attached surface (**b**), spiking concentration of
 668 phenanthrene in sediment (**c**, 10 mg/kg and 20 mg/kg) and incubation time (**d**, 14 d and
 669 28 d: the time of collected samples), respectively. (VN for *Vallisneria natans*; HV for
 670 *Hydrilla verticillata*; SM means submerged macrophytes for VN+ HV; AP for artificial
 671 plants)

672



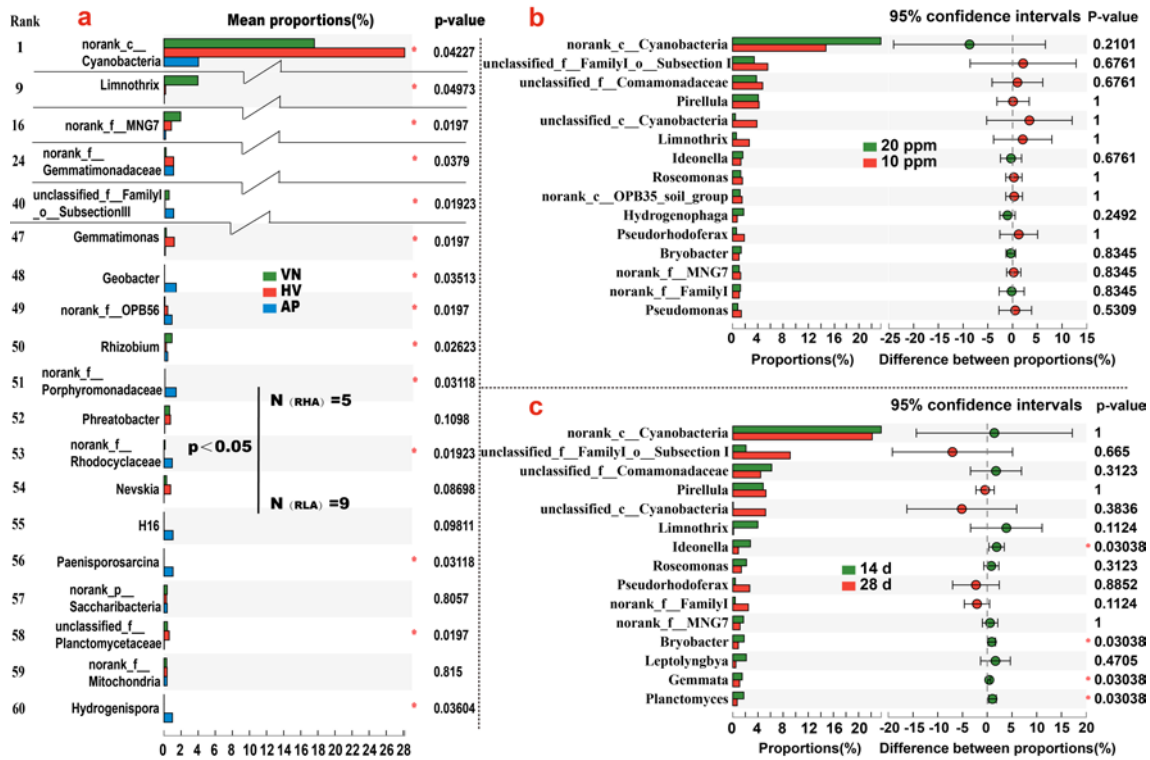
673

674

675 **Fig. 3.** Heat maps of the bacterial community in top 50 genera based on attached surface
 676 (a, AP for artificial plant; HV for *Hydrilla verticillata*; VN for *Vallisneria natans*), spiking
 677 concentration (b, the sediments were spiked by 10 mg/kg and 20 mg/kg phenanthrene)
 678 and incubation time (c, 14 d and 28 d: the time of collected samples). The red corresponds
 679 to higher relative abundance and the green to lower relative abundance.

680

681



682

683 **Fig. 4.** Difference test between genera based on attached surface (**a**, AP for artificial plant;
 684 HV for *Hydrilla verticillata*; VN for *Vallisneria natans*; $N_{(RHA)}$ means the number of
 685 species with relative high abundance; $N_{(RLA)}$ means the number of species with relative
 686 low abundance), spiking concentration (**b**, the sediments were spiked by 10 mg/kg and
 687 20 mg/kg phenanthrene) and incubation time (**c**, 14 d and 28 d: the time of collected
 688 samples).

689 Notes: “*” denotes differences were statistically significant ($p < 0.05$)

690